Check for updates

Biosynthesis of the RiPP trojan horse nucleotide antibiotic microcin C is directed by the *N*-formyl of the peptide precursor†

Shi-Hui Dong, [ID]ab Alexey Kulikovsky,ade Inna Zukher, [ID]d Paola Estrada,a Svetlana Dubiley, [ID]de Konstantin Severinov*def and Satish K. Nair [ID]*abc

Microcin C7 (McC) is a peptide antibiotic modified by a linkage of the terminal isoAsn amide to AMP *via* a phosphoramidate bond. Post-translational modification on this ribosomally produced heptapeptide precursor is carried out by MccB, which consumes two equivalents of ATP to generate the N–P linkage. We demonstrate that MccB only efficiently processes the precursor heptapeptide that retains the *N*-formylated initiator Met (fMet). Binding studies and kinetic measurements evidence the role of the *N*-formyl moiety. Structural data show that the *N*-formyl peptide binding results in an ordering of residues in the MccB "crossover loop", which dictates specificity in homologous ubiquitin activating enzymes. The *N*-formyl peptide exhibits substrate inhibition, and cannot be displaced from MccB by the desformyl counterpart. Such substrate inhibition may be a strategy to avert unwanted McC buildup and avert toxicity in the cytoplasm of producing organisms.

Introduction

Microcin C7 (McC) is a modified heptapeptide, produced by some strains of *E. coli*. The terminal α-carboxylate of McC peptide is conjugated to 5′-phosphate of AMP *via* a phosphoramidate linkage to yield an aspartamide-adenylate that is linked through an N–P bond (Fig. 1).[1,2] McC is a RiPP (ribosomally synthesized and post-translationally modified peptide),[3] wherein the heptapeptide MRTGNAN (**1** or **2**), the product of the *mccA* gene, is modified by the enzyme MccB to yield the adenylate (**3** or **4**).[4,5] The peptide component of McC facilitates both export from the producing strain through MccC major facilitator superfamily membrane transporter and import into susceptible cells *via* the inner membrane YejABEF transporter.[6,7] Upon import into target cells, no-specific proteases cleave the peptide conjugate to release a "warhead" – an inert

analog of aspartyl adenylate **5**, with non-hydrolyzable *N*-acyl phosphoramidate link **6**.[8] The toxin inhibits aspartyl-tRNA synthetase to halt protein synthesis.[9]

The adenylyl transfer reaction catalyzed by MccB consumes two molar equivalents of ATP: the first is used for the attachment of AMP to the α-carboxylate of the MRTGNAN peptide, which subsequently undergoes an intermolecular reaction to form a peptide-succinimide intermediate.[10] Attack of the succinimidyl nitrogen from this intermediate onto the α-phosphate of the second ATP equivalent forms the N–P bond. Hydrolysis of the succinimide ring yields the modified peptide-adenylate in which the terminal Asn encoded by the *mccA* gene is converted to an isoAsn (*i.e.* an aspartamide).[10] Export of the prodrug from the producing organism is carried out by a member of the major facilitator superfamily of membrane transporters (MccC).[4]

Biosynthetic clusters that produce McC-like compounds universally contain only the genes encoding for an MccA-like precursor peptide, the MccB adenylyltransferase and the MccC transporter,[11] but often possess genes that install additional decorations on the peptide aspartamide-adenylate, such as the 3-aminopropyl moiety found on McC **6**.[12,13] Producing strains have developed strategies to avert toxic effects of prematurely processed intact McC (**3** or **4**) in their cytoplasm. Specifically, MccE and MccF carry out either toxin modification or hydrolysis, respectively, to protect against accumulation inside of the host.[14,15]

All RiPP systems must utilize means to guard against the unregulated synthesis of the precursor peptide, which may result in build-up of the modified bioactive product within the cell. In most RiPP systems, this failsafe is ensured by the

aDepartment of Biochemistry, University of Illinois at Urbana-Champaign, Illinois, USA. E-mail: snair@illinois.edu

bCarl Woese Institute for Genomic Biology, University of Illinois at Urbana-Champaign, Illinois, USA

cCenter for Biophysics and Quantitative Biology, University of Illinois at Urbana-Champaign, Illinois, USA

dInstitute of Gene Biology, Russian Academy of Science, 34/5 Vavilo str., 11934 Moscow, Russia

eCenter for Life Sciences, Skolkov Institute of Science and Technology, 3 Nobel str., 143026 Moscow, Russia

fWaksman Institute for Microbiology, 190 Frelinghuysen Road, Piscataway, New Jersey, USA. E-mail: severik@waksman.rutgers.edu

† Electronic supplementary information (ESI) available: Experimental procedures, X-ray crystallographic data, and FP biding curves. See DOI: 10.1039/c8sc03173h
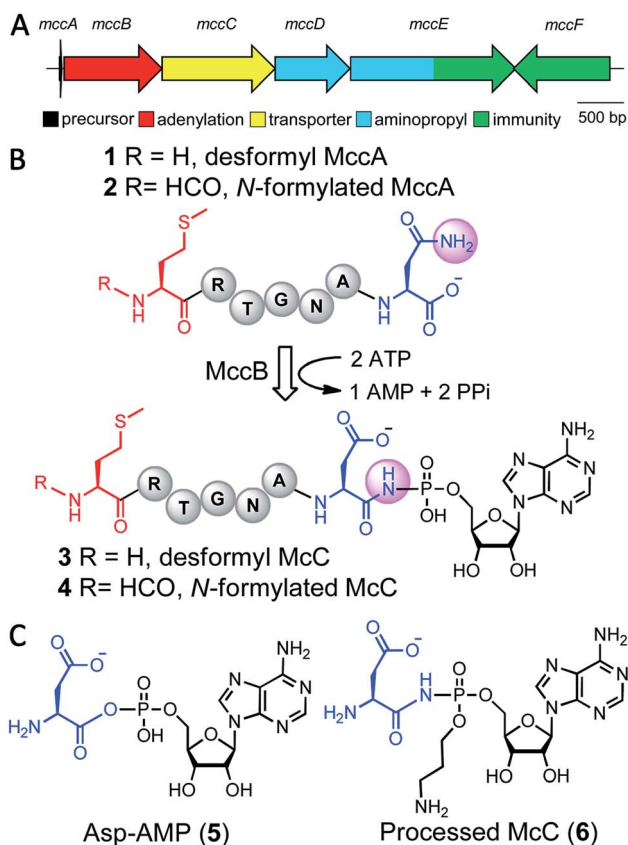
Fig. 1 (A) Biosynthetic gene cluster for the McC toxin from *E. coli*. (B) MccB-catalyzed production of the peptide-adenylate resulting in installation of an N−P linkage. (C) Chemical structures of aspartyl adenylate generated by aspartyl-tRNA. Synthetase (5) and the processed McC toxin (6). Mature McC toxin (6) has a tailoring aminopropyl modification that increases it affinity for the target.
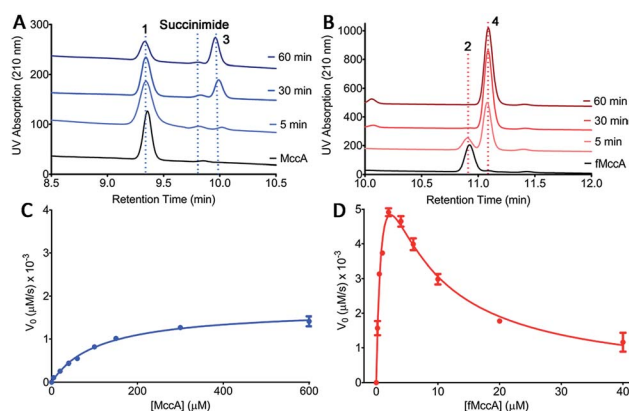
used in the McC biosynthetic pathway, and/or (b) that N-formylation is necessary for toxin export out from producing cells.

In order to distinguish between these two possibilities, we carried out HPLC analysis of the MccB adenylyltransferase-catalyzed reaction products using each 1 and 2 precursor peptides as substrates (Fig. 2A and B). Upon incubation of deformyl peptide 1 (50 μM) with ATP and sub-stoichiometric concentrations of MccB (1 μM), substantial amounts of the substrate remain even after 1 hour, consistent with observations in prior studies using the same desformyl substrate (Fig. 2A).[10,20] In contrast, incubation of N-formylated peptide 2 (50 μM) with the enzyme resulted in the near complete conversion of the substrate after 10 minutes (Fig. 2B). To provide a quantitative assessment of the two substrates, we carried out Michaelis–Menten kinetics of MccB using either 1 or 2 as substrates (Fig. 2C and D).

Consistent with the chromatographic analysis, the catalytic efficiency of MccB using N-formylated 2 (k_{cat}/K_M of 3.6×10^4 M^{-1} s^{-1}) was nearly 12 000 times greater than that with the desformyl 1 peptide (k_{cat}/K_M of 3.0 M^{-1} s^{-1}). Most notably, the kinetic data with N-formylated peptide 2 are consistent with strong substrate inhibition (K_i of ~5.5 μM), as discussed below.

We next sought to understand the molecular rationale underlying the observed four orders of magnitude difference in catalytic efficiency observed with the N-formylated 2 relative to desformyl 1 peptide. To this end, we determined the 1.6 Å resolution co-crystal structure of *E. coli* MccB in complex with ATP, MgCl$_2$ and N-formylated MccA (2) (Fig. 3A; ESI Table S1†). In prior studies,[20] the substrate peptide was directed away from the ATP-binding site. In contrast, our structure presents the MccA substrate bound to MccB in a productive manner consistent with the reaction scheme. Clear and continuous electron density can be observed for the peptide aspartamide-adenylate 4 (generated *in situ*) within the active site (Fig. 3B; ESI Fig. S1†).

The N-formyl moiety is situated in a pocket formed, along one side, by Val240, and Ile243 of one MccB monomer and, on

presence of the leader sequence in the processed substrate, as the bioactive natural product is only elaborated upon removal of the leader peptide by highly specific proteases, typically coupled with extracellular export.[3] Seemingly, no such control point exists for McC, and the catalytic efficiencies of MccE (k_{cat}/K_M of 7.1×10^3 M^{-1} s^{-1})[16] and MccF (k_{cat}/K_M of 3.95×10^4 M^{-1} s^{-1})[17] for toxin inactivation may not be sufficient to overcome toxic buildup of 6 within the producing cell. Thus, McC biosynthesis may be regulated by other means.

Results and discussion

The initial characterization of intact McC purified from a producing strain showed that the molecule lacked a free α-amino group.[18] Subsequent structural elucidation of the isolated product using ^{1}H NMR was consistent with N-formylation of the initiator Met of the peptide conjugate 4.[5] Moreover, systematic analysis of substrate scope of the YejABEF importer that internalizes intact McC into target cells demonstrated that 4 was a significantly better substrate than the peptide that lacked the N-formyl moiety 3.[19] These data are consistent with two possibilities: (a) that only the N-formylated precursor 2 is

Fig. 2 (A and B) HPLC analysis of the time-course of the MccB reaction progress using either (A) desformyl MccA 1 or (B) N-formylated MccA 2 as a substrate. (C and D) Michaelis–Menten kinetics curves for MccB with either (C) 1 or (D) 2 as a substrate. Error bars represent standard deviation of the mean ($n = 3$).
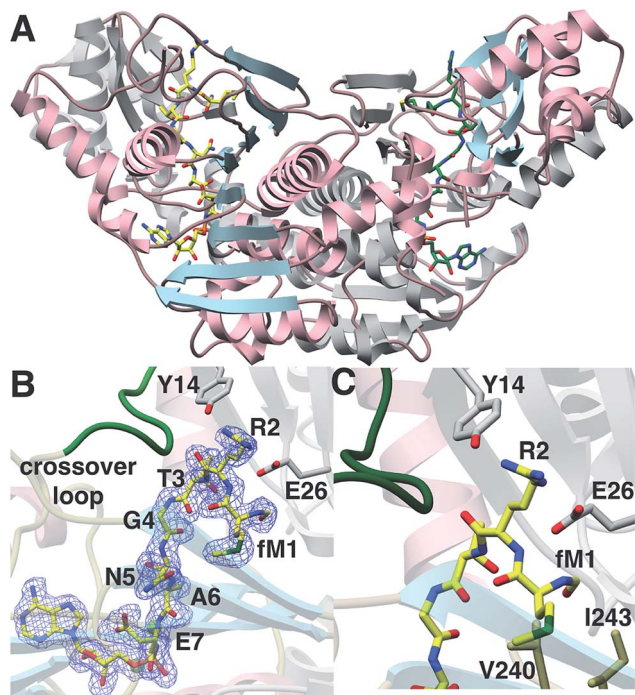
Fig. 3 (A) Structure of MccB homodimer bound to product **4**. One monomer is colored in gray and the other in pink and blue. (B) Coordinates of the MccB-**4** complex superimposed on a difference Fourier map ($F_{obs} - F_{calc}$) contoured at 2.5σ using phases from the final model with the coordinate of **4** removed prior to a round of simulated annealing refinement. (C) Close-up view of the N-formyl binding pocket of MccB.

Table 1 FP and competition FP binding data of MccB variants binding to the N-formylated **2** substrate

Variant	K_d (μM)	IC_{50} (μM)	K_i (μM)	[Protein] (μM)
Y14A	143.40 ± 35.90	NA	NA	NA
E26A	91.11 ± 4.70	NA	NA	NA
E26D	539.40 ± 358.40	NA	NA	NA
E26Q	16.93 ± 3.11	59.34 ± 8.75	13.46	30
S212A	2.06 ± 0.05	6.99 ± 1.02	2.87	2
F217A	8.85 ± 0.88	32.07 ± 7.36	11.86	10
I243A	>800	NA	NA	NA
V264A	79.17 ± 12.81	682.50 ± 61.55	399.29	50
Y268A	17.57 ± 1.80	93.35 ± 15.65	37.28	20
Y268F	4.15 ± 0.37	36.83 ± 3.18	15.14	5
H333A	5.01 ± 0.37	26.55 ± 2.98	11.62	5

the other side, by Gly23 and Glu26 from the other monomer (Fig. 3C). The formyl oxygen is engaged with the backbone of Gly23 and the side chain of Glu26. Perhaps as a result of the productive binding mode for **4**, electron density can also be observed of residues Lys262 through Lys271, which correspond to the "crossover loop" that connects the two active sites in homologous ubiquitin-like protein activating enzymes (E1) (ESI Fig. S2†). These newly observed contacts reveal that a number of residues located within the "crossover loop" engage in interactions with the MccA peptide.

In order to validate the interactions with product observed in the crystal structure, we analyzed the binding of wild-type MccB to fluorescein isothiocyanate (FITC) labeled peptide (**2**) that is not a substrate, yielding a $K_d \sim 3.6$ μM (ESI Table S2 and Fig. S3 and S4†). Competition fluorescence polarization assays using unlabeled **2** yields a $K_i \sim 9$ μM. We next tested a panel of variants of MccB with amino acid substitutions at both the N-formyl site, and at the crossover loop (Table 1; ESI Table S3 and Fig. S5–S7†). Removal of part of the N-formyl binding pocket in the Ile243 → Ala variant results in near complete loss of binding to **2**. Likewise, Ala mutation at residues along the Lys262–Lys271 crossover loop severely compromises binding, as is seen in Val264Ala ($K_d \sim 79$ μM), and Tyr268Ala ($K_d \sim 18$ μM) MccB derivatives, with substitutions of residues that line the peptide-binding pocket (ESI Fig. S2†). These data affirm the role of the crossover loop in reinforcing productive binding of the

MccA substrate. The specificity of complementary interactions between a given E1 activating enzyme and its cognate ubiquitin-like protein (Ubl) substrate is a hallmark of the Ubl activation.[21–24]

In order to gain additional inferences regarding MccB substrate specificity based on homologous Ubl conjugation systems, we carried out comparative analysis with the structure of eukaryotic E1s, namely those of Uba1 in complex with ubiquitin, Sae2 in complex with SUMO, and Uba3 in complex with NEDD8 (ESI Fig. S2†).[21–24] In each of these structures, the residue corresponding to Arg72 in ubiquitin affects substrate recognition *via* complementary interactions with residues in the crossover loop of the cognate E1.[24] In our co-crystal structure, Arg2* (the asterisk designates the numbering of residues in the substrate) from the N-formylated precursor **4** is directed towards the peptide binding clamp in the adjacent monomer, where Tyr14 forms platform along one edge, and Glu26 wedges in between the N-formyl oxygen of fMet1* and the guanidino group of Arg2* (Fig. 3C). The importance of these residues is highlighted by the nearly 40-fold increase in K_d (~143 μM) for Tyr14 → Ala, and 25-fold increase in K_d (~91 μM) for Glu26 → Ala MccB (Table 1; ESI Fig. S5†).

As our kinetic measurements of MccB suggested substrate inhibition (K_i of ~5.5 μM) by the N-formylated **2**, but not with the desformyl **1** peptide, we analyzed differences in binding to MccB in greater detail using competition fluorescence polarization (FP) assays with FITC-labeled precursor peptides. Label-free N-formylated **2** was able to efficiently compete with the labeled peptide ($K_i \sim 9$ μM) (Fig. 4A). In contrast, FITC-labeled desformyl **1** only weakly bound to MccB with a K_d of ~378.7 μM (ESI Fig. S4 and S8†). Notably, desformyl **1** could not displace bound FITC-labeled N-formylated **2**, even at concentrations greater than 5 mM (Fig. 4A), while N-formylated **2** was able to displace FITC-labeled desformyl **1** with a $K_i \sim 52$ μM (ESI Fig. S9†). Hence, N-formylation of the MccA precursor enables substrate inhibition of MccB.

Based on our structural data, we hypothesized that the interactions established between Glu26 in MccB and the fMet1* and Arg2* of **2** may contribute to substrate inhibition. In order to test this theory, we carried out Michaelis–Menten kinetics of Glu26 → Ala MccB using N-formylated **2** as a substrate. This
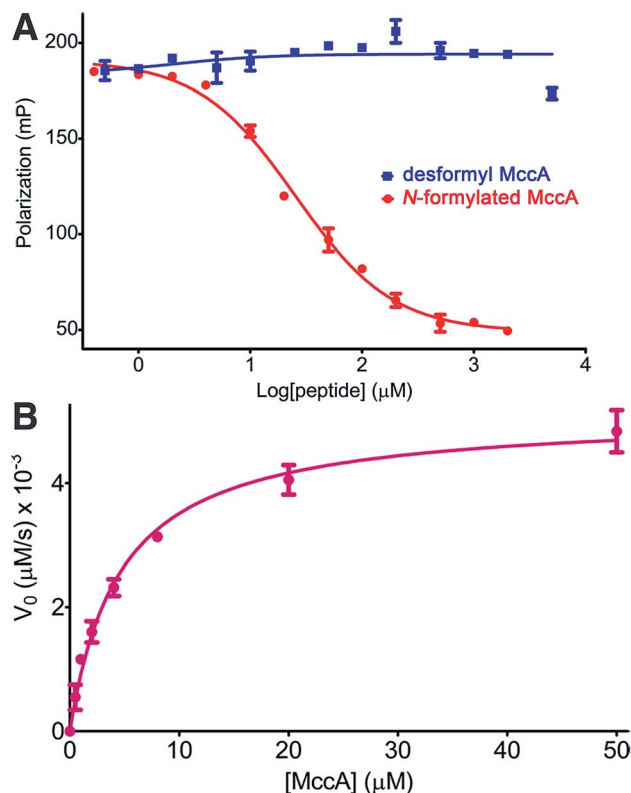
Fig. 4 (A) Competition FP binding curves of MccB using FITC labeled *N*-formylated **2** as probe. (B) Michaelis–Menten kinetics curve for Glu26 → Ala MccB with *N*-formylated **2** as substrate. Error bars represent standard deviation of the mean ($n = 3$).

variant demonstrated a 33-fold decrease in catalytic efficiency (k_{cat}/K_M of 1.1×10^3 M^{-1} s^{-1}) (Fig. 4B). More importantly, no substrate inhibition by **2** was observed with Glu26 → Ala MccB, confirming that the interactions between Glu26 of MccB, and fMet1* and Arg2* of **2** play a role in mediating substrate inhibition (Fig. 3C). Hence, Arg2* plays a role analogous to that of Arg72 in ubiquitin in establishing the specificity of MccB with the *N*-formylated MccA precursor peptide.

Conclusions

The inhibition of enzymatic turnover at high concentrations of substrate is prevalent throughout primary metabolism, and occurs across various classes of catalysts.[25] Our studies highlight a rare example of the use of substrate inhibition in a natural product biosynthetic pathway. We have previously demonstrated that an intrinsic transcription terminator located between the *mccA* and *mccB*, coupled with a ribosome-mediated stabilization of the monocistronic *mccA* transcript results in a 20-fold excess of the precursor peptide, relative to the MccB adenylase.[26] The role of the interaction between Glu26 and fMet1* and Arg2* of **2** in mediating substrate inhibition is notable as similar interactions are conserved across various classes of E1-like activating enzyme and cognate substrates. When the MccC-mediated efflux becomes saturated, production of excess product **4** may result in processing and cellular

toxicity, given that the immunity determinants have catalytic efficiencies in the order of $\sim 10^4$ M^{-1} s^{-1}. Substrate inhibition limits this unwanted situation, and excess production with most RiPP natural products cellular toxicity is minimal, as the leader peptide, required for post-translational modifications, must be removed for bioactivity to appear. However, this is not the case with McC as intracellular processing of endogenous **4** will liberate active toxin **6** within the producing organism. Thus, inhibition of MccB by substrate **2** may restrict overproduction of **4** providing an expedient means to avert the unwanted buildup of a toxic metabolite within the producing organism at conditions of excess precursor peptide synthesis or decreased export of mature compound.

Conflicts of interest

The authors declare no competing financial interest.

Acknowledgements

References

1 K. Severinov and S. K. Nair, *Future Microbiol.*, 2012, **7**, 281–289.

2 K. Severinov, E. Semenova, A. Kazakov, T. Kazakov and M. S. Gelfand, *Mol. Microbiol.*, 2007, **65**, 1380–1394.

3 P. G. Arnison, M. J. Bibb, G. Bierbaum, A. A. Bowers, T. S. Bugni, G. Bulaj, J. A. Camarero, D. J. Campopiano, G. L. Challis, J. Clardy, P. D. Cotter, D. J. Craik, M. Dawson, E. Dittmann, S. Donadio, P. C. Dorrestein, K. D. Entian, M. A. Fischbach, J. S. Garavelli, U. Goransson, C. W. Gruber, D. H. Haft, T. K. Hemscheidt, C. Hertweck, C. Hill, A. R. Horswill, M. Jaspars, W. L. Kelly, J. P. Klinman, O. P. Kuipers, A. J. Link, W. Liu, M. A. Marahiel, D. A. Mitchell, G. N. Moll, B. S. Moore, R. Muller, S. K. Nair, I. F. Nes, G. E. Norris, B. M. Olivera, H. Onaka, M. L. Patchett, J. Piel, M. J. Reaney, S. Rebuffat, R. P. Ross, H. G. Sahl, E. W. Schmidt, M. E. Selsted, K. Severinov, B. Shen, K. Sivonen, L. Smith, T. Stein, R. D. Sussmuth, J. R. Tagg, G. L. Tang, A. W. Truman, J. C. Vederas, C. T. Walsh, J. D. Walton, S. C. Wenzel, J. M. Willey and W. A. van der Donk, *Nat. Prod. Rep.*, 2013, **30**, 108–160.

4 J. E. Gonzalez-Pastor, J. L. San Millan, M. A. Castilla and F. Moreno, *J. Bacteriol.*, 1995, **177**, 7131–7140.

5 J. I. Guijarro, J. E. Gonzalez-Pastor, F. Baleux, J. L. San Millan, M. A. Castilla, M. Rico, F. Moreno and M. Delepierre, *J. Biol. Chem.*, 1995, **270**, 23520–23532.

6 T. Kazakov, A. Metlitskaya and K. Severinov, *J. Bacteriol.*, 2007, **189**, 2114–2118.

7 M. Novikova, A. Metlitskaya, K. Datsenko, T. Kazakov, A. Kazakov, B. Wanner and K. Severinov, *J. Bacteriol.*, 2007, **189**, 8361–8365.

8 T. Kazakov, G. H. Vondenhoff, K. A. Datsenko, M. Novikova, A. Metlitskaya, B. L. Wanner and K. Severinov, *J. Bacteriol.*, 2008, **190**, 2607–2610.

9 A. Metlitskaya, T. Kazakov, A. Kommer, O. Pavlova, M. Praetorius-Ibba, M. Ibba, I. Krasheninnikov, V. Kolb, I. Khmel and K. Severinov, *J. Biol. Chem.*, 2006, **281**, 18033–18042.

10 R. F. Roush, E. M. Nolan, F. Lohr and C. T. Walsh, *J. Am. Chem. Soc.*, 2008, **130**, 3603–3609.

11 O. Bantysh, M. Serebryakova, K. S. Makarova, S. Dubiley, K. A. Datsenko and K. Severinov, *mBio*, 2014, **5**, e01059-14.

12 A. Kulikovsky, M. Serebryakova, O. Bantysh, A. Metlitskaya, S. Borukhov, K. Severinov and S. Dubiley, *J. Am. Chem. Soc.*, 2014, **136**, 11168–11175.

13 A. Metlitskaya, T. Kazakov, G. H. Vondenhoff, M. Novikova, A. Shashkov, T. Zatsepin, E. Semenova, N. Zaitseva, V. Ramensky, A. Van Aerschot and K. Severinov, *J. Bacteriol.*, 2009, **191**, 2380–2387.

14 M. Novikova, T. Kazakov, G. H. Vondenhoff, E. Semenova, J. Rozenski, A. Metlytskaya, I. Zukher, A. Tikhonov, A. Van Aerschot and K. Severinov, *J. Biol. Chem.*, 2010, **285**, 12662–12669.

15 A. Tikhonov, T. Kazakov, E. Semenova, M. Serebryakova, G. Vondenhoff, A. Van Aerschot, J. S. Reader, V. M. Govorun and K. Severinov, *J. Biol. Chem.*, 2010, **285**, 37944–37952.

16 V. Agarwal, A. Metlitskaya, K. Severinov and S. K. Nair, *J. Biol. Chem.*, 2011, **286**, 21295–21303.

17 V. Agarwal, A. Tikhonov, A. Metlitskaya, K. Severinov and S. K. Nair, *Proc. Natl. Acad. Sci. U. S. A.*, 2012, **109**, 4425–4430.

18 J. F. Garcia-Bustos, N. Pezzi and C. Asensio, *Biochem. Biophys. Res. Commun.*, 1984, **119**, 779–785.

19 G. H. Vondenhoff, B. Blanchaert, S. Geboers, T. Kazakov, K. A. Datsenko, B. L. Wanner, J. Rozenski, K. Severinov and A. Van Aerschot, *J. Bacteriol.*, 2011, **193**, 3618–3623.

20 C. A. Regni, R. F. Roush, D. J. Miller, A. Nourse, C. T. Walsh and B. A. Schulman, *EMBO J.*, 2009, **28**, 1953–1964.

21 D. T. Huang, H. W. Hunt, M. Zhuang, M. D. Ohi, J. M. Holton and B. A. Schulman, *Nature*, 2007, **445**, 394–398.

22 I. Lee and H. Schindelin, *Cell*, 2008, **134**, 268–278.

23 L. M. Lois and C. D. Lima, *EMBO J.*, 2005, **24**, 439–451.

24 B. A. Schulman and J. W. Harper, *Nat. Rev. Mol. Cell Biol.*, 2009, **10**, 319–331.

25 M. C. Reed, A. Lieb and H. F. Nijhout, *BioEssays*, 2010, **32**, 422–429.

26 I. Zukher, M. Novikova, A. Tikhonov, M. V. Nesterchuk, I. A. Osterman, M. Djordjevic, P. V. Sergiev, C. M. Sharma and K. Severinov, *Nucleic Acids Res.*, 2014, **42**, 11891–11902.